Supporting information

Persistent Quantum Coherence and Strong Coupling Enable Fast Electron Transfer across CdS/TiO_2 Interface: a Time-domain Ab Initio Simulation

Hamid Mehdipour,[†] Alexey V. Akimov,[‡] Joanna Jankowska,[#] Ali T. Rezakhanai,[†] Saeedeh. S. Tafreshi,[†] Nora H. de Leeuw,[||] Alireza Z. Moshfegh,[†,†,*] Oleg V. Prezhdo,[#,*]

[†]Department of Physics, Sharif University of Technology, Tehran, Iran.

[‡]Department of Chemistry, University at Buffalo, The State University of New York, Buffalo, New York 14260-3000, United States

[#]Department of Chemistry, University of Southern California, Los Angeles, California 90089, United States

[||]School of Chemistry, Cardiff University, Main Building, Park Place, Cardiff, CF10 3AT, UK

[†]Institute for Nanoscience and Nanotechnology, Sharif University of Technology, Tehran, Iran.

*Address correspondence to *moshfegh@sharif.edu*; *prezhdo@usc.edu*

This **Supporting Information** file includes:

- **Theoretical Methodology**
- **Figure S1-S6**
- **Optimized CdS(110)/TiO_2(101) supercell, and CdS and TiO unit cells**
- **References**

Theoretical Methodology

The dynamics of photo-induced charges is simulated using nonadiabatic molecular dynamic based on the well-known decoherence-induced surface hopping view of a mixed quantum-classical system of nuclei and electrons.[1] Time-domain density functional theory is employed to formulate the probability of hopes between electronic energy surfaces (as a result of interaction with nuclei environment).[2]

Time-Domain Density Functional Theory

Similar to time-independent density functional theory (DFT) of Kohn-Sham, time-domain DFT (TDDFT) employs concept of total electron density to describe the electronic properties of a system.[3] In TDDFT, the electron density is time-dependent and is expressed by the sum of the occupied time-dependent single-electron orbitals, $\varphi_i(\mathbf{r}, t)$:

$$n(\mathbf{r}, t) = \sum_{i=1}^{N} |\varphi_i(\mathbf{r}, t)|^2, \tag{1}$$

where N is the total number of electrons. The time-dependent orbitals are determined by the application of the time-dependent variational principle to the total KS energy density functional subject to the normalization constraint on the orbitals.[3] Each time-dependent single-electron orbital $\varphi_i(\mathbf{r}, t)$ satisfies the equation

$$i\hbar \frac{\partial \varphi_i(\mathbf{r}, t)}{\partial t} = H(\mathbf{r}, \mathbf{R}, t)\varphi_i(\mathbf{r}, \mathrm{R}). \tag{2}$$

In the above equation $H(\mathbf{r}, \mathbf{R}, t)$ is a functional of the total density. As a result, the electronic subsystem is described by N equations coupled through the density. The electron orbitals are coupled to the lattice vibrations through the electrostatic potential in H. Equation (2) is solved by expanding the time-dependent single-electron orbital in terms of adiabatic KS orbitals, which can be obtained for each set of nuclear coordinates,

$$\varphi_i(\mathbf{r}, t) = \sum_j c_j(t)\, \tilde{\varphi}_j(\mathbf{r}, t) \tag{3}$$

By inserting the above expansion in Eq. (2), the time-dependent Schrodinger equation is turned into a time evolution equation for expansion coefficient:

$$i\hbar \frac{\partial}{\partial t} c_j(t) = \sum_k c_k(t) \left(\epsilon_k \delta_{jk} + \boldsymbol{d}_{jk}.\dot{\mathbf{R}}\right) \tag{4}$$

where ϵ_k is the energy of the adiabatic state k, $\boldsymbol{d}_{jk}$ is nonadibatic coupling vector and $\dot{\mathbf{R}}$ is classical particle velocity. $\boldsymbol{d}_{jk}.\dot{\mathbf{R}}$ ($\boldsymbol{D}_{ij}$) is obtained numerically over a time step by applying the approach of Hammes-Schiffer and Tully.[4]

$$D_{jk}\left(t + \frac{dt}{2}\right) = -i\hbar \left\langle \tilde{\varphi}_j \middle| \frac{\partial}{\partial t} \middle| \tilde{\varphi}_k \right\rangle \approx -\frac{i\hbar}{2\Delta t}\left(\left\langle \tilde{\varphi}_j(t) \middle| \tilde{\varphi}_k(t+\Delta t)\right\rangle - \left\langle \tilde{\varphi}_j(t+\Delta t) \middle| \tilde{\varphi}_k(t)\right\rangle\right) \tag{5}$$

Fewest Switches Surface Hopping

Detailed balance between the upward and downward energy transition is required to obtain correct dynamic of electronic subsystem and its energy exchange with lattice vibrations. FSSH of Tully provides rational procedure to achieve such objective for mixed quantum-classical systems.[5] It introduces the concept of probability of transition (hopping) between states based on the evolution of expansion coefficients, Eq (4). The probability of a hope from state *i* to state *j* within the time interval dt is given by

$$dP_{ij} = \frac{b_{ij}}{a_{ij}} dt, \tag{6}$$

where

$$a_{ij} = c_i(t)c_j(t), \quad b_{ij} = 2\hbar^{-1}\mathrm{Im}\left(a_{ij}\langle \tilde{\varphi}_i | H | \tilde{\varphi}_j \rangle\right) - 2\mathrm{Re}\left(a_{ij}\boldsymbol{d}_{ij}\right). \tag{7}$$

If the time-dependent hopping probability dP_{ij} is negative, it is set to zero. Also, a hope from state *i* to state *j* can only occur when following condition is met:

$$\sum_{k=0}^{j-1} P_{i\to k}(t) < \xi \leq \sum_{k=0}^{j} P_{i\to k}(t), \tag{8}$$

where ξ is a random number between 0 and 1. The condition (8) means that the hope is possible only when the occupation of state *i* decreases and the occupation of state *j* increases. To account for conservation of electron-nuclear energy after each eligible hope, the FSSH algorithm rescales the nuclear velocities along the direction of the nonadibatic coupling vector, $\boldsymbol{d}_{jk}$. If a quantified transition to higher energy electronic system is predicted based on the above conditions, but the kinetic energy available along $\boldsymbol{d}_{jk}$ is not sufficient to accommodate the electronic energy increase, the electronic hope is rejected. Therefore, the velocity rescaling and hope rejection give the detailed balance between the upward and downward energy transitions, mimicking the Boltzmann statistic and providing the condition of quantum-classical thermodynamics equilibrium.[6]

The FSSH uses the classical path approximation (CPA) that keeps the nuclear dynamics unaffected by the dynamics of the electronic degrees of freedom and only the electronic dynamics is driven by motion of nuclei (lattice vibrations). The electronic Hamiltonian is a function of the classical nuclear coordinates of a MD trajectory. The MD trajectory is computed for ground-state electronic state and thus is completely independent of the electronic transitions. Therefore, this approximation makes the FSSH of transition simple and computationally efficient.[7] It also produces a time-dependent potential that drives numerous FSSH realizations of electronic dynamics using only a single MD trajectory.

Decoherence-Induced Surface Hopping

Despite simplicity and computational time-saving aspects of FSSH-CPA, it fails to properly describe the quantum effects of the mixed classical-quantum system since wavepacket nature of lattice vibration is neglected in it. Quantum decoherence is an importanteffect that occurs for each pair of states as a result of elastic interactions of electronic-subsystem and

lattice vibration.[1, 8] Lattice vibrations can randomize relative phase of the electronic states and cause decoherence of states from each other. It becomes more important when loss of coherence occur much faster than the electronic transition. Loss of coherence could be a true cause of hops between different electronic states, decoherence-induced surface hopping (DISH).[1] The quantum coherence time for a pair of states depends strongly on the magnitude of the nuclear-induced fluctuations of the energy gap of the two states.[8] The phonon-induced decoherence rate associated with quantum electronic transitions is estimated using the optical response theory in which pure-dephasing time stands as the decoherence time for a pair of states.[9]

The pure-dephasing time for each pair of states is calculated according to the following procedure.[9] The fluctuations in the energy difference of the states is characterized by the normalized energy gap autocorrelation function (n-ACF):

$$C(t) = \frac{\langle \delta E(t) \delta E(0) \rangle_T}{\langle \delta E(0)^2 \rangle_T}, \tag{9}$$

The brackets denote averaging over a canonical ensemble. Here, $\delta E(t) = \Delta E_{ij}(t) - \langle \Delta E_{ij}(t) \rangle$ is the fluctuation of the energy difference between states *i* and *j* from its average value $\langle E_{ij}(t) \rangle$. The ACF quantifies the correlation between the electronic states energy levels and nuclear modes coupled to the electronic subsystem. In another way, it characterizes the memory of the energy gap fluctuations. Very large initial gap fluctuations $\langle \delta E(0)^2 \rangle_T$ indicates a very fast pure dephasing of the electronic states.[8]

The pure-dephasing function is calculated using second-order cumulant expansion to the optical response function:[9]

$$D_{cumu}(t) = \exp\big(-g(t)\big) \tag{10}$$

where $g(t)$

$$g(t) = \int_0^t dx \int_0^x dy C(y). \tag{11}$$

Fitting the D_{cumu} by Gaussian function $\exp(-0.5(t/\tau)^2)$ gives the pure-dephasing time.

The vibration spectral density responsible for energy gap fluctuations is obtained by taking Fourier transform of ACF as follows:

$$I(\omega) = \left| \frac{1}{\sqrt{2\pi}} \int_{-\infty}^{\infty} dt e^{-i\omega t} C(t) \right|^2 \tag{12}$$

After simulation time evolved to the decoherence time of the pair of states, the corresponding probability of each state (square of expansion coefficient, $|c_i(t)|$) of the two states are evaluated and by using a sequence of random numbers sampled from the Poisson distribution the coefficient with the lower value is reset to zero.

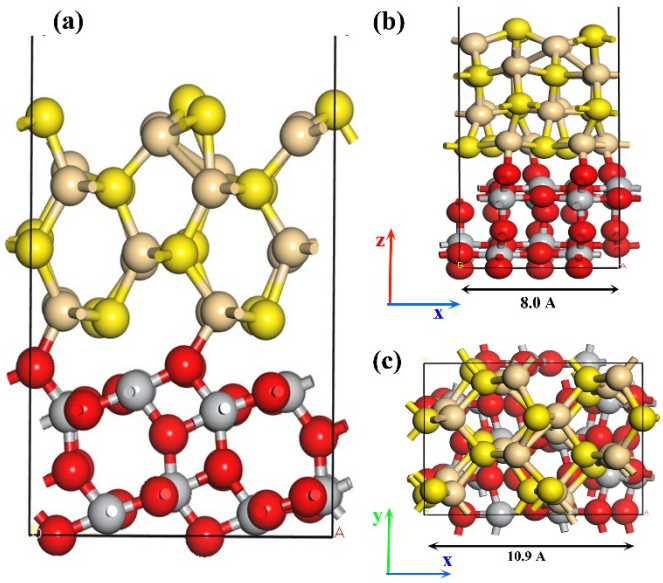

Figure S1: Relaxed geometry of CdS(110)/TiO_2(101) interface at temperature $T = 0\ K$ from x (a), y (b), and z (c) directions.

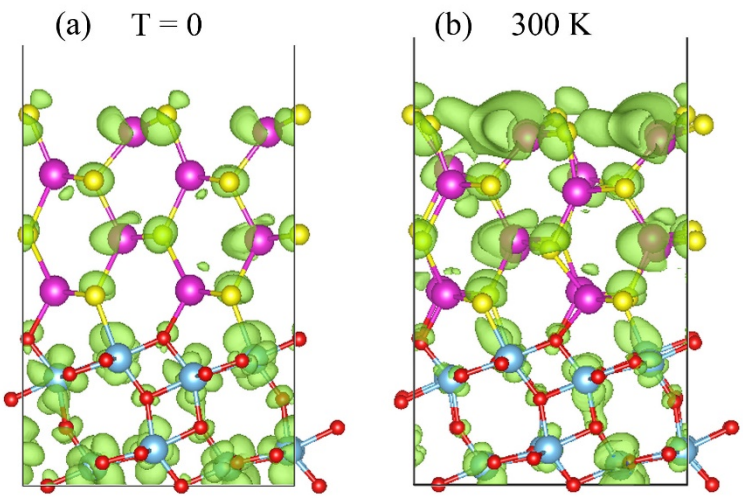

Figure S2: Charge density of donor state in ET process at temperatures **(a)** $T = 0$ and **(b)** $T = 300\ K$. The isosurface is set at 0.0002 for both panels. Enhanced delocalization of electron charge density along the bond line connecting atoms of the donor and acceptor systems is observed.

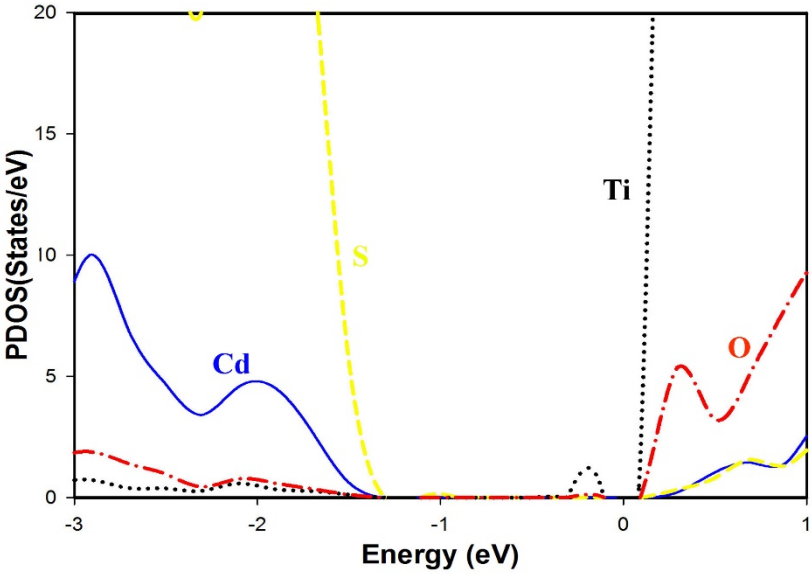

Figure S3: Atom-projected density of states (APDOS) for the CdS/TiO_2 interface at temperature $T = 300\ K$. APDOS of Cd, S, Ti and O atoms are shown with solid blue, dashed yellow, dotted black, and dash-dottted red curves, respecteively. The Fermi energy is set at zero.

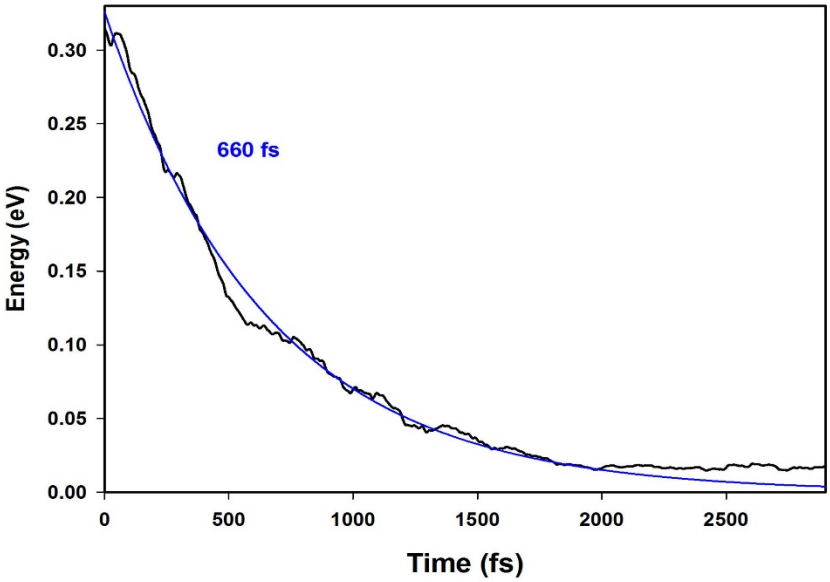

Figure S4: Evolution of energy of the photo-excited electron transfering across the CdS/TiO_2 junction. The time constant is obtained by exponential fitting, $f(t) = exp(-t/\tau)$.

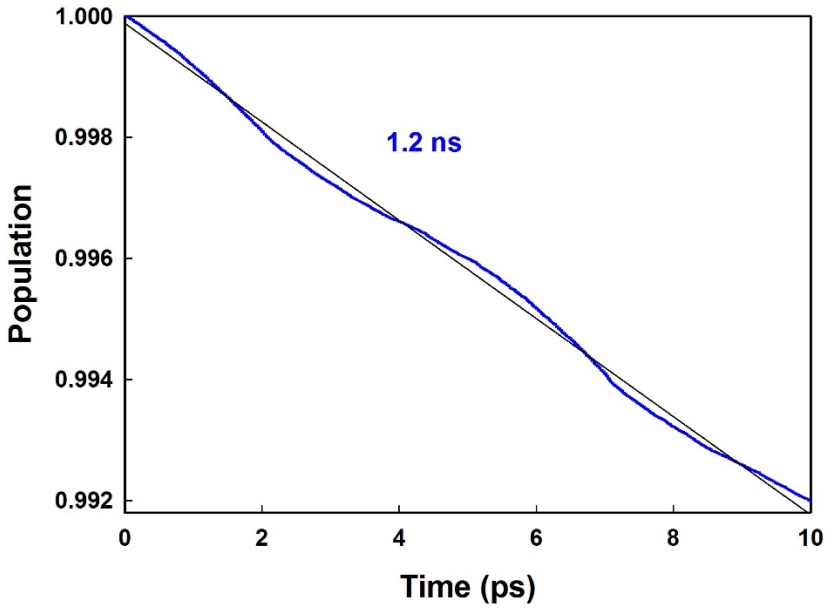

Figure S5: Evolution of population of LUMO in pure CdS. The time constant is obtained using the short-time linear approxiation to exponential decay, $f(t) = exp(-t/\tau) \approx 1 - t/\tau$.

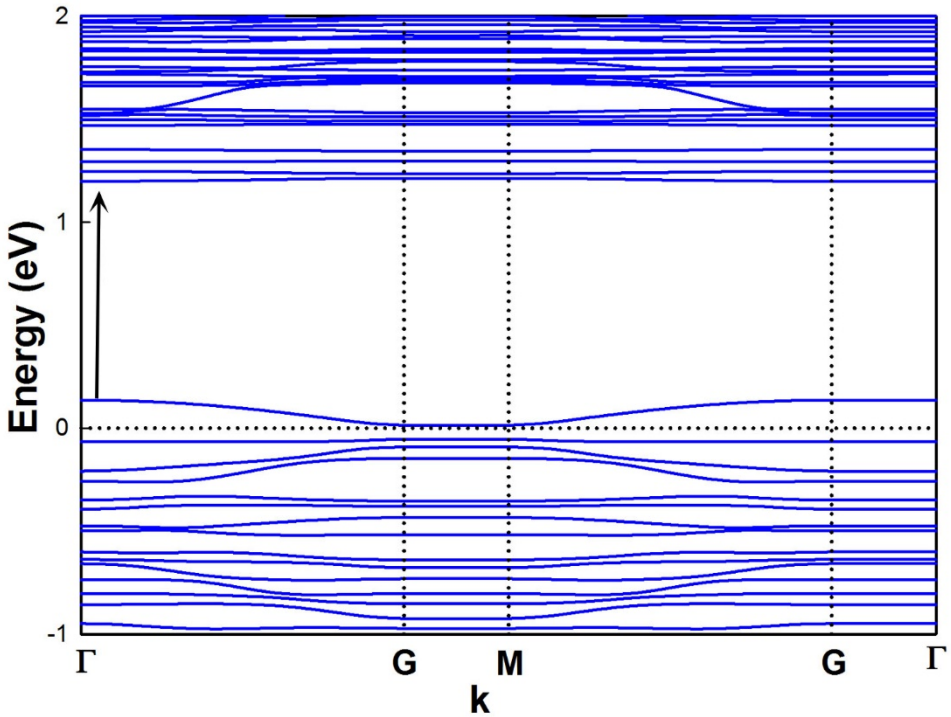

Figure S6: Band structure of the CdS/TiO_2 heterostructure.

Optimized CdS(110)/TiO_2(101) supercell

Table S1: Optimized Cartesian atomic positions of the CdS(110)/TiO_2(101) interface. Orthorhombic, $a = 10.9$ Å, $b = 8$ Å, $c = 40$ Å, (80 atoms).

Atom	x	y	z
Ti	2.831567627	6.020493787	0.756390492
Ti	8.227619598	3.958840396	0.756390492
Ti	8.204388821	0.041035074	0.756390492
Ti	2.808338335	2.010620365	0.756390492
Ti	10.609678225	2.039910814	1.418050851
Ti	9.280977951	2.087599051	4.955585837
Ti	9.289871729	6.005750830	5.012243790
Ti	10.666487126	5.947219099	1.498620327
Ti	1.470812549	5.867050527	4.291674068
Ti	1.380925473	1.972701217	4.202595396
Ti	3.871925831	3.907191625	5.023374056
Ti	6.849203579	4.054967135	4.255129816
Ti	5.155594142	3.891927388	1.529589820
Ti	3.803663179	0.034551147	4.972878563
Ti	6.858135155	0.187443798	4.283311949
Ti	5.174210122	-0.031838008	1.524029764
O	0.982449435	2.025828427	0.000000000
O	6.374828115	3.994549048	0.000000000
O	6.351596994	-0.005325739	0.000000000
O	1.005680654	6.035702807	0.000000000
O	3.194646847	-0.006091180	0.912560007
O	3.217877828	3.993783291	0.912560007
O	8.628429178	5.999393529	0.912560007

Table S1: continued from previous page

O	8.605197350	1.989519330	0.912560007
O	10.101369111	0.162066970	1.356143840
O	8.748587240	0.140163785	4.948543576
O	10.476274059	2.273586391	3.396765867
O	10.177018487	4.022571333	1.174091207
O	7.376202009	2.083207311	4.555792221
O	8.810233498	4.073419794	4.877837624
O	7.333294582	6.023413481	4.498512825
O	10.498537705	6.162073118	3.489761648
O	0.176768309	5.602039076	5.793482947
O	4.685432575	5.848790489	1.384410948
O	1.638905347	5.800529714	2.305508841
O	3.360121975	5.854175896	4.850862773
O	3.316258019	1.956149261	4.858876583
O	5.680691555	4.160714811	5.802290879
O	1.996991628	3.860537409	4.439040293
O	5.016158234	3.700494699	3.492906901
O	1.503301305	1.859637202	2.212746328
O	7.023606653	3.998704772	2.259255371
O	4.710265165	1.956376096	1.349833052
O	0.183064106	1.760126450	5.726478833
O	5.584524271	0.377282429	5.848653123
O	1.934129500	0.022420428	4.294660883
O	5.046744401	-0.041178511	3.481243107
O	7.027486562	0.244426050	2.326331792
Cd	1.164532581	1.840458534	7.698500092

Table S1: continued from previous page

Cd	1.103632477	5.510278867	7.846030474
Cd	6.685258082	4.397578759	7.721297510
Cd	6.864962929	0.733997052	7.713240292
Cd	3.937117396	6.991551503	9.496448640
Cd	4.005194298	3.399559569	9.732356939
Cd	9.444128246	3.105558825	9.943453881
Cd	9.265811087	6.796891664	9.767341598
Cd	1.404223365	5.126942991	12.524745175
Cd	1.396305782	1.114209485	12.012735342
Cd	6.530791536	1.199087774	11.953527306
Cd	6.699070282	5.216450411	12.451378838
Cd	9.806337202	7.213922113	13.955512808
Cd	9.703507801	3.040774960	13.772840945
Cd	4.673974119	3.156119566	13.729960642
Cd	4.627902149	7.264344503	13.905053630
S	2.894035161	3.764508588	7.478465438
S	2.491550693	7.584849123	7.503895087
S	8.269853891	6.361088333	7.590204348
S	8.541032856	2.604292187	7.451944437
S	5.380389172	1.257785554	9.699017661
S	5.761177930	5.171373019	9.912875948
S	0.122613125	1.041326787	9.841399823
S	0.125215228	4.974759883	10.195064978
S	3.070001433	6.982339655	11.934648843
S	2.987263322	3.202618012	11.970826771
S	8.086799686	3.180512736	11.951755829

Table S1: continued from previous page

S	8.243989172	7.158249916	11.945075867
S	-0.020128018	5.068931997	14.689234237
S	0.473798229	1.262789906	14.344927748
S	5.679713137	5.105219783	14.847626130
S	6.343019236	1.288919256	14.445053781

Optimized anatase TiO_2 simulation cell

Table S2: Optimized Cartesian atomic positions of anatase TiO_2. Tetragonal, $a = b = 7.53$ Å, $c = 10.0$ Å (48 atoms).

Atom	x	y	z
Ti	1.879924114	5.647344182	5.028543796
Ti	-0.001959973	5.658140198	2.513393813
Ti	3.763396425	5.658163972	2.513599709
Ti	5.645014434	5.652489625	5.028528277
Ti	5.644991194	1.887372791	5.028618694
Ti	5.645994042	0.005255917	7.543901649
Ti	5.645980139	3.770360096	7.543785087
Ti	3.763567699	0.010855160	-0.001265029
Ti	3.763378148	1.893057772	2.513700349
Ti	3.763569151	3.775956044	-0.001364725
Ti	-0.001797956	3.775939105	-0.001603728
Ti	1.880879606	3.765215223	7.543315099
Ti	-0.001977765	1.893040679	2.513482939
Ti	-0.001789716	0.010833242	-0.001490758
Ti	1.880886124	0.000112929	7.543412628
Ti	1.879895162	1.882237729	5.028642751
O	1.880141692	5.648972800	7.057318919
O	-0.002890896	5.657435997	0.484452554
O	1.880546186	5.649845857	2.998431170
O	-0.002103734	5.657030676	4.542258440
O	3.761901812	5.657056136	4.542509303
O	3.765298612	5.657456894	0.484678161
O	5.645626248	5.653964549	3.000829851

Table S2: continued from previous page

O	5.645244710	5.653899393	7.057669108
O	5.646353570	0.006425675	9.571513292
O	5.643957996	0.006257412	5.514800433
O	5.645210149	1.888793850	7.057761666
O	5.645608089	1.888840693	3.000902443
O	5.646348164	3.771557469	9.571406423
O	5.643947892	3.771361690	5.514683883
O	3.762874493	0.010182975	8.029707261
O	3.765283896	1.892359489	0.484760846
O	3.765505612	0.009927729	2.027727537
O	3.761886995	1.891924676	4.542607529
O	3.762873764	3.775293123	3.775293123
O	3.765501732	3.775023834	2.027641760
O	-0.002699516	3.775006401	2.027426790
O	-0.001142221	3.775254419	8.029382781
O	1.878848290	3.766436496	5.514564126
O	1.881249272	3.767437686	9.573325241
O	-0.002134642	1.891905782	4.542351713
O	1.880525305	1.884732959	2.998545177
O	-0.002685248	0.009905577	2.027515746
O	-0.002923809	1.892342027	0.484535577
O	-0.001129101	0.010158013	8.029494205
O	1.880105365	1.883870610	7.057432457
O	1.878839233	0.001341274	5.514667390
O	1.881252868	0.002341797	9.573439763

Optimized CdS simulation cell

Table S3: Optimized Cartesian Atomic positions of CdS. Orthorhombic unit cell, $a = 11.26$ Å, $b = 8.68$ Å, $c = 8.68$ Å, (32 atoms).

Atom	x	y	z
Cd	5.636314126	-0.046771729	4.339802811
Cd	2.816352715	2.134724628	6.515658065
Cd	0.006717385	-0.048359047	4.340478301
Cd	8.449221019	2.117145411	6.515395281
Cd	2.822395438	6.483217386	6.518450341
Cd	8.454492728	6.466360353	6.518371137
Cd	8.453873541	6.465099803	2.170113884
Cd	8.448606480	2.116248724	2.166930027
Cd	0.007042428	-0.049120526	-0.008395902
Cd	5.636923962	-0.047522168	-0.008205947
Cd	0.006954304	4.300395314	4.343219837
Cd	5.636496190	4.303201382	4.342578926
Cd	0.007477861	4.299706653	-0.005142540
Cd	2.816331541	2.133820956	2.167393245
Cd	2.822289447	6.482048200	2.170440915
Cd	5.637109765	4.302280095	-0.004752001
S	1.411549364	-0.039261034	6.515375381
S	4.226268662	2.126584347	4.341849151
S	1.411522969	-0.040403545	2.167219422
S	7.042898357	-0.053597641	2.166924260
S	9.856054059	2.131572121	4.341421334
S	7.042685946	-0.052298251	6.514956669
S	7.044766737	4.294624996	6.517930609

Table S3: continued from previous page

S	1.412655657	4.307492235	6.518160076
S	4.225872076	6.474552988	4.343981696
S	9.856181918	6.480471129	4.343528891
S	7.045140845	4.293915588	2.169142724
S	9.855949041	2.131011863	-0.007176490
S	9.856325911	6.479722220	-0.004385607
S	4.225884141	6.473806242	-0.004409250
S	4.226260649	2.126126628	-0.007033593
S	1.412840980	4.306948207	2.169198617

References:

(1) Jaeger, H. M.; Fischer, S.; Prezhdo, O. V., Decoherence-Induced Surface Hopping. *J. Chem. Phys.* **2012**, *137*, 22A545-1-13.

(2) Craig, C. F.; Duncan, W. R.; Prezhdo, O. V., Trajectory Surface Hopping in the Time-Dependent Kohn-Sham Approach for Electron-Nuclear Dynamics. *Phys. Rev. Lett.* **2005**, *95*, 163001-1-4.

(3) Runge, E.; Gross, E. K. U., Density-Functional Theory for Time-Dependent Systems. *Phys. Rev. Lett.* **1984**, *52*, 997-1000.

(4) Hammes-Schiffer, S.; Tully, J. C., Proton Transfer in Solution: Molecular Dynamics with Quantum Transitions. *J. Chem. Phys.* **1994**, *101*, 4657-4667.

(5) Tully, J. C., Molecular Dynamics with Electronic Transitions. *J. Chem. Phys.* **1990**, *93*, 1061-1071.

(6) Parandekar, P. V.; Tully, J. C., Mixed Quantum-Classical Equilibrium. *J. Chem. Phys.* **2005**, *122*, 094102-1-6.

(7) Akimov, A. V.; Prezhdo, O. V., The Pyxaid Program for Non-Adiabatic Molecular Dynamics in Condensed Matter Systems. *J. Chem. Theory. Comput.* **2013**, *9*, 4959-4972.

(8) Akimov, A. V.; Prezhdo, O. V., Persistent Electronic Coherence Despite Rapid Loss of Electron–Nuclear Correlation. *J. Phys. Chem. Lett.* **2013**, *4*, 3857-3864.

(9) Mukamel, S., *Principles of Nonlinear Optical Spectroscopy*; Oxford University Press: New York Oxford, U. S. A, **1999**.